

Ultra Efficient Internal Shocks

Shiho Kobayashi¹ and Re'em Sari²

¹Department of Earth and Space Science, Osaka University, Toyonaka, Osaka 560, Japan

²Theoretical Astrophysics 130-33, California Institute of Technology, Pasadena, CA 91125, USA

ABSTRACT

Gamma-ray bursts are believed to originate from internal shocks which arise in an irregular relativistic wind. The process has been thought to be inefficient, converting only a few percent of the kinetic energy into gamma-rays. We define ultra efficient internal shocks as those in which the fraction of emitted energy is larger than the fraction of energy given to the radiating electrons at each collision. We show that such a scenario is possible and even plausible. In our model, colliding shells which do not emit all their internal energy are reflected from each other and it causes subsequent collisions, allowing more energy to be emitted. As an example, we obtain about 60% overall efficiency even if the fraction of energy that goes to electrons is $\epsilon_e = 0.1$ provided that the shells' Lorentz factor varies between 10 and 10^4 . The numerical temporal profile reflects well the activity of the source which ejects the shells, though numerous collisions take place in this model.

Subject headings: gamma rays: bursts; shock waves; relativity

1. Introduction

A widely accepted mechanism for producing a cosmological gamma-ray burst (GRB) is the deceleration of relativistically expanding shells. The kinetic energy of the shells is converted into internal energy by relativistic shocks. These shocks can be due to collision with the ambient medium (external shocks) or shocks inside the shell itself due to nonuniform velocity (internal shocks). Electrons are heated by the shocks, and the internal energy is radiated via synchrotron and IC emission, with broken power law spectra (e.g. Sari, Piran and Narayan 1998).

Most bursts have a highly variable temporal profile with variability time scale significantly shorter than the overall duration. In the external shocks scenario this

variability is due to irregularity in the surrounding material, but the efficiency is extremely low (Fenimore, Madras & Nayakshin 1996; Sari & Piran 1997). Thus, GRBs are believed to be produced by the other alternative: internal shocks. The inner engine itself should be variable in this scenario, the observed temporal profile follows very closely the operation of the source (Kobayashi, Piran & Sari 1997, KPS97 hereafter). Using a simple model, we have estimated that the hydrodynamic efficiency of this process (transforming kinetic energy to internal energy) is about 10% .

Kumar (1999) argued that the conversion efficiency from the bulk motion to gamma-ray is only 1%. His argument is based on three points: (I) The hydrodynamic efficiency is, as mentioned above, typically 10%. (II) It is only the electrons that are radiating. Even in equipartition among protons, magnetic field and electrons, the latter electrons only have a third of the internal energy. (III) The amount of the radiated energy within the gamma-ray band is about a third of the total radiated one. Combining these three factors give the low efficiency of $\frac{1}{10} \times \frac{1}{3} \times \frac{1}{3} = 1\%$.

Such a low efficiency results in sever energy demands on the source. Moreover, it has problems explaining the energy ratio between the GRB and its afterglow. According to the internal-external shock model, the remaining kinetic energy, which was not converted to radiation by internal shocks, is radiated during the afterglow stage. External shock does not suffer from problem (I), and the energy released in the afterglow should be considerably higher than that in the GRBs. However, it seems to be that the energy during the afterglow is only a tenth of that during the GRB, rather than ten times larger (Frontera et. al. 2000, Kumar & Piran 2000, Freedman & Waxman 2000). Even though the observational constraints are not very good since most of the energy is released at very early radiative stages where the afterglow was not observed, a factor of ten more energy in the afterglow seems to be excluded.

A possible solution to these problems is to assume large angular fluctuation in the shells (Kumar and Piran 1999). This model has clear predictions in the form of afterglow variability whose amplitude decay in time. It also predicts that the afterglow may be sometimes more energetic than the GRBs.

In this paper, we suggest a simple alternative solution, which overcomes the problems suggested by Kumar. We show that if the distribution of the Lorentz factor is not uniform, but instead its logarithm is distributed uniformly, then the typical ratio of Lorentz factors between neighboring shells is considerably larger. Then, the hydrodynamic efficiency can be close to hundred percents, even for a reasonable spread of Lorentz factors (Similar calculation was recently done by Beloborodov 2000). The main point of this paper is the possibility of “ultra-efficient” internal shocks. We define ultra-efficient internal shocks as

a scenario in which the emitted fraction of kinetic energy is larger than ϵ_e , the fraction of internal energy that is going into electrons (and then radiated) at each collision. We will show that such a scenario is possible and even reasonable.

2. “Ultra Efficient” Internal Shocks

Internal shocks could occur within a variable relativistic wind produced by a highly variable source. We represent the irregular wind by a succession of relativistic shells with a random distribution of Lorentz factors in a similar manner as in KPS97. Beloborodov (2000) has shown that the internal shocks can convert most of the kinetic energy to internal energy if the fluctuation of the initial Lorentz factors $A^2 = (\langle \gamma^2 \rangle - \langle \gamma \rangle^2) / \langle \gamma \rangle^2$ is large. Though it is maximally 1/3 if the initial Lorentz factors take random values between γ_{min} and γ_{max} , it is not limited if the distribution is uniform in logarithmic space between $\log \gamma_{min}$ and $\log \gamma_{max}$.

The efficiency can be estimated by an equation similar to equation 19 in KPS97. The most efficient case is that the masses of the shells are taken equal, and that the efficiency is given by a simple form:

$$\langle \epsilon \rangle \sim 1 - a^{1/2} \log a / (a - 1) \quad (1)$$

where $a = \gamma_{max} / \gamma_{min}$. The efficiency is plotted as a function of the fluctuation $A^2 = -1 + (a + 1) \log a / 2(a - 1)$ in figure 1. This analytic estimate fits the result of our numerical simulation, and has the asymptotic form $\langle \epsilon \rangle = A^2 / 2$ which Beloborodov estimated for a small fluctuation. Our expression above generalizes Beloborodov estimate and gives reasonable estimate of the efficiency also for large fluctuations.

Though we have seen that a large hydrodynamic efficiency is possible if the fluctuation of the initial Lorentz factors is large, it is not reasonable that all the internal energy is emitted after each collision, since electrons do not have most of the internal energy. Defining ϵ_e as the fraction of energy given to electrons we expect $\epsilon_e < 1$. Even at equipartition with protons $\epsilon_e = 1/2$. Under these circumstances the total emitted energy in Beloborodov model is still limited by ϵ_e .

However, if $\epsilon_e < 1$ the merger produced by a collision is expected to stay hot after the emission. As a result, the merger will spread to transform the remaining internal energy back to the kinetic energy (Kumar 1999). A simplified description of this process is to assume that the two shells reflect with a smaller relative velocity. The difference of the kinetic energy before and after the collision is the emitted internal energy. The reflecting shell will collide into the other neighbor shell. Since in this way a large amount of collisions

are caused, the overall efficiency from the kinetic energy to the radiation could be larger than ϵ_e . This is the key ingredient of our model. Before going on with this model, we present some hydrodynamic simulations which shows that these simplified assumptions are reasonable.

3. Hydrodynamic Simulation

To estimate the conversion efficiency of the internal shocks process, it is important to understand how high velocity shells interact with slower ones and dissipate the the kinetic energy. We consider here a collision of two equal mass shells with very different Lorentz factors, $\gamma_r/\gamma_s \gg 1$. The rapid and the slower shells are denoted by the subscriptions r and s respectively. We assume that the widths of the shells are comparable in the ISM rest frame. This is a reasonable assumption since in this frame, the width is given directly by the “inner engine”. Even so, the width of the rapid shell \hat{l}_r is much larger when viewed from the rest frame of the rapid shell $\hat{l}_r/\hat{l}_s \sim (\gamma_r/\gamma_s)^2/2$. Then, the dense “slower” shell with Lorentz factor $\hat{\gamma}_s \sim \gamma_r/2\gamma_s$ collides into the low density “rapid” shell in this frame, $\rho_s/\rho_r \sim \gamma_r/\gamma_s$. This is a planar analog of the evolution of a relativistic fireball (Sari & Piran 1995, Kobayashi, Piran and Sari 1999). When it begins to interact with the surrounding material, two shocks are formed: a forward shock propagating into the rapid shell and a reverse shock propagating into the slower one. After the reverse shock crosses the slower shell, the profile of the shocked rapid shell material approaches to that of its fireball analog: the “blast wave” which sweeps and collects the surrounding material. Once the shock wave crosses the rapid shell, the hydrodynamical structure is as follows. There is a shocked rapid shell, the analog of the “blast wave” and the shocked slow shell, which cooled down and is the analog of the adiabatically cooling “fireball ejecta”. The structure of such a system in the fireball case was studied by Sari and Piran 1999 and Kobayashi and Sari 2000.

Since $\hat{\gamma}_s^2 \gg \rho_s/\rho_r$, the slow shell is considerably decelerated by the relativistic reverse shock down to $\sim (\gamma_r/\gamma_s)^{3/4}$ and heated to a relativistic temperature at the crossing time $t_s \sim (\gamma_r/\gamma_s)^{3/2}\hat{l}_s/c$. Then, it cools adiabatically and follows a planar version of the Blandford Mckee (1976) solution (Sari 2000), in which a given fluid element evolves with a bulk Lorentz factor of $\gamma \propto l^{-3/2}$. Therefore, the motion becomes Newtonian $\gamma \sim (\gamma_r/\gamma_s)^{3/4}(t_r/t_s)^{-3/2} \sim 1$ when the forward shock crosses the rapid shell at $t_r = \hat{l}_r/c$. On the other hand, since the forward shock itself evolves as $\gamma \propto l^{-1/2}$, it slows down to $\gamma \sim (\gamma_r/\gamma_s)^{1/2}/2$ at the crossing time t_r .

We have developed a relativistic code with an exact Riemann solver to solve relativistic hydrodynamics problems (Kobayashi, Piran & Sari 1999). Using this code, we numerically

study the collision of two equal mass slabs with $\gamma_s = 10$, $\gamma_r = 10^3$ and the same width in the ISM frame. The initial condition in the rapid shell comoving frame is

$$\begin{aligned} \hat{\gamma}_r &= 1 & \hat{\gamma}_s &\sim 50 \\ \rho_r &= 1 & \rho_s &= 100 \\ \hat{l}_r &\sim 5000 & \hat{l}_s &= 1 \end{aligned}$$

The mass density outside the slabs and the homogeneous pressure are $\rho = 10^{-8}$ and $p = 10^{-10}$. The mass density and the pressure are measured in the comoving frame of each fluid. Our adiabatic simulations represent a case in which ϵ_e is very small. In this simulation, we used the unit of $c = 1$.

To compare the analytical estimates with the numerical simulation we define the effective Lorentz factor of each shell as $\langle \gamma \rangle = \int m \gamma dl / \int m dl$ with the effective mass $m = \gamma \{ \rho + (3 + \beta^2) p \}$. The numerical simulation then gives $\langle \hat{\gamma}_r \rangle \sim 5.3$ and $\langle \hat{\gamma}_s \rangle \sim 1.6$ at the crossing time, which are in agreement with the analytical estimates. The thin line in figure 6 shows the numerical density profile at this time. After the forward shock crosses the rapid shell, a rarefaction wave begins to propagate into the rapid shell to transform the internal energy to the kinetic, then the rapid is accelerated to $\gamma \sim \gamma_r / 2 \gamma_s$. The center of mass moves with a Lorentz factor $\sim (\gamma_r / \gamma_s) / 2 \sim 5$ in the rapid shell comoving frame. At the end of the simulation $t = 10^5$, about forty percent of the rapid shell material is slower than the center of mass, and goes with the slower shell (see fig 2b).

4. Two Shell Collision

A collision of two shells is the elementary process in our model. A rapid shell catches up a slower one and the two merge to temporarily form a single one (denoted by the subscript m). Using conservation of energy and momentum, the Lorentz factor of the merged shell γ_m and the internal energy E_{int} produced by the collision are given by

$$\gamma_m \sim \sqrt{(m_r \gamma_r + m_s \gamma_s) / (m_r / \gamma_r + m_s / \gamma_s)}, \quad E_{int} = m_r (\gamma_r - \gamma_m) + m_s (\gamma_s - \gamma_m). \quad (2)$$

After a fraction ϵ_e of the internal energy is emitted isotropically in the local frame of merged shell (center of mass frame), the shells will spread to transform the remaining internal energy back to kinetic energy. If the widths are the same in center of mass frame, each mass is conserved before and after the collision. However, as we have seen, some fraction of the rapid shell material goes together with the slower one after the collision in

general. We parameterize the mass splitting as $m'_r = (1 - \delta)m_r$ and $m'_s = m_s + \delta m_r$. We later show that the total efficiency is not sensitive to δ .

The Lorentz factor of the reflected shells in center of mass frame are given by

$$\bar{\Gamma}_r = (M^2 + m_r'^2 - m_s'^2)/2m_r'M, \quad \bar{\Gamma}_s = (M^2 + m_s'^2 - m_r'^2)/2m_s'M. \quad (3)$$

where $M = (m_r\gamma_r + m_s\gamma_s - \epsilon_e E_{int}/c^2)/\gamma_m$. The Lorentz factors in laboratory frame are

$$\Gamma_r = \bar{\Gamma}_r\gamma_m - \sqrt{(\bar{\Gamma}_r^2 - 1)(\gamma_m^2 - 1)}, \quad \Gamma_s = \bar{\Gamma}_s\gamma_m + \sqrt{(\bar{\Gamma}_s^2 - 1)(\gamma_m^2 - 1)}. \quad (4)$$

The shells are once compressed by shocks, but these spread when reflecting. For simplicity we assume that the width of the shells, l_i , is constant.

5. Multiple Shell Collision

We consider a wind consisting of N shells. Each shell is characterized by the four variables: γ_i, m_i, l_i and R_i . We assume that the initial Lorentz factor of each shell is distributed uniformly in logarithmic space between $\log \gamma_{min}$ and $\log \gamma_{max}$. The initial masses are assumed to be correlated with the Lorentz factors as $m \propto \gamma^\eta$. For $\eta = -1$ and 0 the shells initially have equal energy and equal mass respectively, and for $\eta = 1$ the shells initially have equal density under an assumption of the equal shell width. We assume a constant value l for the initial widths and the initial separations between the shells. Then, the initial position of the shells are $R_i = 2(i - 1)l$.

The evolution of the system in time is basically same as in KPS97, but equation 4 is used to calculate the Lorentz factor of the reflecting shells for the next time step. We follow the evolution of shells until there are no more collisions, i.e. until the shells are ordered with increasing value of the Lorentz factors.

The conversion efficiency from the kinetic energy of the shells to radiation can be calculated by using the initial and final kinetic energy as $\langle \epsilon \rangle = 1 - \Sigma m_i^{(f)} \gamma_i^{(f)} / \Sigma m_i^{(i)} \gamma_i^{(i)}$ where the superscripts (f) and (i) represent the initial and final values respectively. It depends on the model parameters $\{\gamma_{max}/\gamma_{min}, N, \eta, \epsilon_e, \delta\}$ and on the specific realization: the set of random Lorentz factors assigned to each shell. For each choice of the parameters of the model, we have evaluated the efficiency for 100 realizations. The mean efficiency and its standard deviation are listed in Table 1 for the conserved equal mass case ($\eta = \delta = 0$).

Table.1

N	γ_{min}	γ_{max}	efficiency [%] ($\epsilon_e = 0.1$)	efficiency [%] ($\epsilon_e = 0.5$)
30	10^2	10^3	9.2 ± 2.3	16.2 ± 3.0
30	10	10^4	40.0 ± 9.2	67.5 ± 9.3
10^2	10^2	10^3	15.1 ± 1.5	17.7 ± 1.5
10^2	10	10^4	62.9 ± 4.8	72.4 ± 4.3

The efficiency approaches an asymptotic value as the Lorentz factor ratio $\gamma_{max}/\gamma_{min}$ and the number of the shells N increase. The asymptotic value depends on η , ϵ_e and δ . The efficiency is plotted in fig 3 as a function of η for $\delta = 0, 0.4$ or 0.8 . In the range $-1 \leq \eta \leq 1$, it is not very sensitive to δ and peaks around $\eta \sim 0$, i.e. the most efficient case is the equal mass case.

The efficiency is plotted as a function of ϵ_e for the conserved equal mass case ($\eta = \delta = 0$) in Figure 4. It is interesting that the efficiency can be larger than ϵ_e since the energy released in GRB can be much larger than that in the afterglow. For instance, consider the case of $N = 100$, $\gamma_{min} = 10$, $\gamma_{max} = 10^4$, $\eta = \delta = 0$ and $\epsilon_e = 0.1$, the internal shocks can convert about sixty percent of the kinetic energy to the radiation. The reminder is converted to the thermal energy by external shock. However, only the fraction $\epsilon_e = 0.1$ of that is emitted as the afterglow ¹, the efficiency by the external shock is only four percent. The GRB to the afterglow ratio for these parameters is about 15!

Figure 5a shows the resulting temporal structure in the equal mass case. It is a superposition of pulses from the elementary two shell collisions. Though numerous collisions take place during the evolution, the number of peaks in the profile is of order of N . Since all peaks have widths of the same order of magnitude, the different amplitude of the peaks originates mainly from the difference in the internal energy produced by the collisions. In Figure 5b, we plot the initial Lorentz factor as a function of time when shells were emitted by the source. We evaluate E_{int} for all pairs of the shells if inner shell is faster. We assign E_{int} to the ejection time of the inner shell (see Figure 5c). It resembles well the temporal profile in 5a. Therefore, despite the complicated nature of the two shells collisions, the observed burst closely follows the inner engine temporal profile.

Neighboring shells collide on a time scale of $2\gamma^2 l/c$. The matter is moving toward the observer, the resulting observer time scale is l/c . On the other hand, the difference in observer time due to the location of the given shell within the wind is of order Nl/c . Then, we observe the pulses arising from the collisions according to their positions inside the wind. In Figure 5d we plot the shell's index against the time when a radiation from the

¹In fact, Sari 1997 have shown that also during the afterglow the fraction of energy that can be emitted may exceed ϵ_e . However, this will be spread over many decades of time.

shell is observed. Although the light curve in figure 5a is the superposition of all pulses, in figure 5d we plot only the pulses which are higher than a tenth of the highest. We can see a clear correlation between the index and the time, the temporal profile reflects the activity of the source.

The deviation from the correlation, e.g. some groups of circles in a line from left top to right bottom is due to that a rapid inner shell collides into the outer neighbor, and the boosted shell further collides into the outer. Since the masses of the shells are equal, the Lorentz factors of the inner and the outer shells are just switched at each collision if the radiation is negligible. Then, if an initial Lorentz factor of a shell is peculiarly high, the index of the shell which has the high Lorentz factor propagates outwards. In this sequence with the radiation loss, the pulse from the collisions damps quickly, then, the overall correlation is not destroyed.

The temporal structures for equal energy cases ($\eta = -1$) are plotted in figure 6. The merger at each collision is assumed to split to the original masses (figure 6a) or to the modified masses $\delta = 0.4$ (figure 6c). The initial distributions of γ are the same with that of figure 5. For $\eta = -1$, E_{int} takes almost the same value for most of the collisions (KPS97), so most of the peaks have comparable amplitudes. The profiles still reflect the activity of the source well.

6. Conclusions

We have shown that the conversion efficiency from kinetic energy of relativistic shells to radiation can be close to hundred percent if the source produces shells with comparable masses with different Lorentz factor, especially when the logarithms of the Lorentz factors are distributed uniformly (see also Beloborodov 2000). It had been assume in our previous work that the Lorentz factors themselves were distributed uniformly, and the efficiency was less than forty percent. With this distribution, the most efficient case is that the source produces shells with comparable energy, instead of comparable masses (KPS97).

However, this high efficiency is achieved assuming that all the internal energy is emitted at each collision, this is not reasonable since only electrons radiative effectively, and these do not have all the internal energy. After the electrons radiate, large amount of the internal energy remains in protons. Using a hydrodynamic simulation, it has been shown that the hot merger produced by a collision spreads to transform the remaining internal energy back to the kinetic one. A simplified description of this process is to assume that the shells reflect each other with a smaller relative velocity, after the collision. The difference of the

kinetic energy gives the radiated internal energy.

Since the reflecting shell collide into the outer neighbor shell, the index of the shell which has a high Lorentz factor propagates outerwards until the high value decays by the radiation loss. The shell itself which has initially a high Lorentz factor might not go through many collisions, but its high “kinetic energy” does. Therefore, the internal shock process is very efficient even if the fraction of internal energy emitted at each collision is small. Previously, the efficiency in the case of $\epsilon_e < 1$ had been estimated as smaller by a factor of ϵ_e than that in the corresponding fully radiative case. Our ultra efficient internal shocks scenario shows this to be a significant underestimate. Though the efficiency that we have estimated is bolometric efficiency, the efficiency from the kinetic energy of the shells to gamma-ray radiation is also high if the fraction of the energy radiated in the BATSE band is not very small.

Numerous collisions happened in our ultra-efficient internal shocks model, it made the peak width wider than in the previous internal shocks model. However, the number of main peaks is still almost the same as the number of shells that the source emitted. There is a strong correlation between the time at which we observe a pulse and the emission time of the corresponding shell from the source. This correlation persists even for a small ϵ_e case where larger number of collision happen. The temporal structure reproduces the activity of the source.

We have shown that the efficiency of the internal shock process is not limited by ϵ_e , while that of the external shock is so. If a fraction ζ of kinetic energy of an explosion is converted to the radiation by the internal shocks, all the remaining one is converted to the thermal by external shock in the afterglow stage, and a fraction ϵ_e of the thermal is emitted. Then, we can roughly estimate the ratio between the energy released in afterglow and that in GRB as $\sim \epsilon_e(1 - \zeta)/\zeta$. Assuming $\epsilon_e = 0.1$, the ratio is 1/10 for $\zeta = 0.5$ and decrease as ζ increase. If the efficiency of internal shocks is indeed very large, the luminosities of GRB and the afterglow are expected to be anticorrelated.

As a general argument in internal shock model, the luminosity distribution of multi peak bursts would be narrower than that of bursts with only few peaks (Kumar & Piran 2000), since the number of the peaks is almost the number of the shells N as we have shown. We verified that the dispersion of the efficiency is proportional to $1/\sqrt{N}$ in our numerical model.

S.K. acknowledges support from the Japan Society for the Promotion of Science. R.S. acknowledges support from the Sherman Fairchild foundation.

References

- Beloborodov,A. 2000, ApJL, 539, L25.
Fenimore,E.E., Madras,C.D. & Nayakshin,S. 1996,ApJ,437,998.
Freedman,D.L. & Waxman,E. 1999, Submitted to ApJ, astro-ph/9912214.
Frontera F., et. al., 2000, ApJS, 127, 59.
Kobayashi,S., & Sari,R. 2000, ApJ, 542, 819.
Kobayashi,S., Piran,T. & Sari,R. 1997, ApJ, 490, 92.
Kobayashi,S., Piran,T. & Sari,R. 1999, ApJ, 513, 669.
Kumar, P. 1999, ApJL, 523, 113.
Kumar, P. & Piran,T. 2000, ApJ, 535, 152.
Sari,R. 1997, ApJL, 489, L37.
Sari,R 2000 in preparation.
Sari,R. & Piran,T. 1997, ApJ, 485, 270.
Sari,R., Piran,T. & Narayan R. 1998, ApJL, 497, L17.

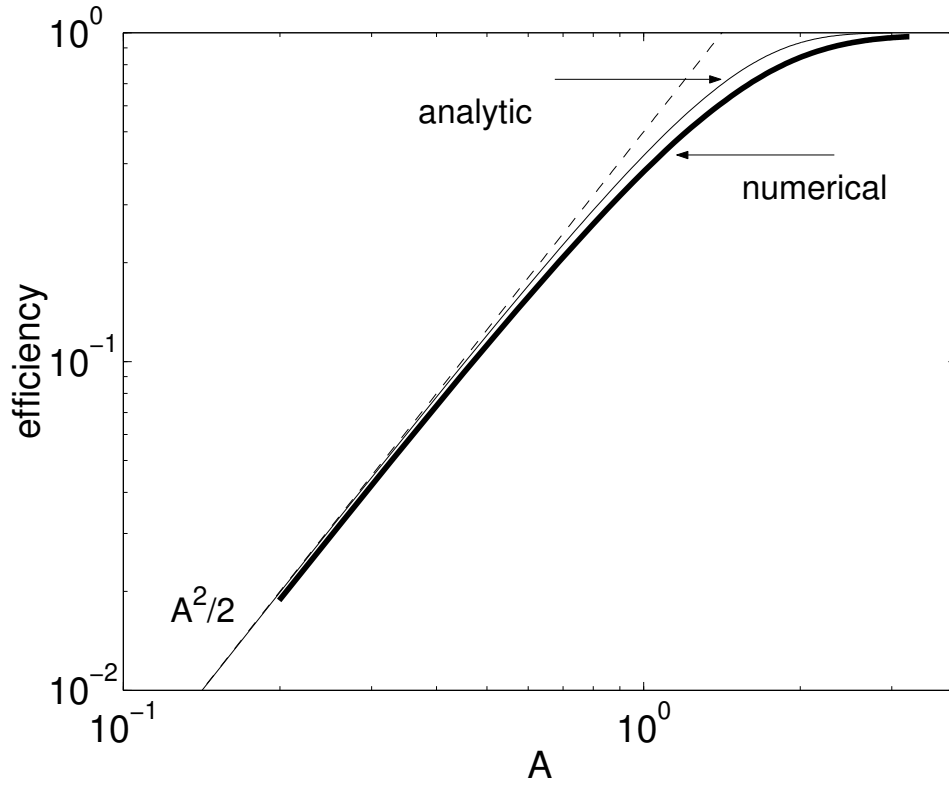


Fig. 1.— Fully radiative case ($\epsilon_e = 1$): efficiency vs A . thick solid (numerical simulation: average of 100 random simulations with 100 equal mass shells), thin solid (analytic estimate), dashed ($\langle \epsilon \rangle = A^2/2$)

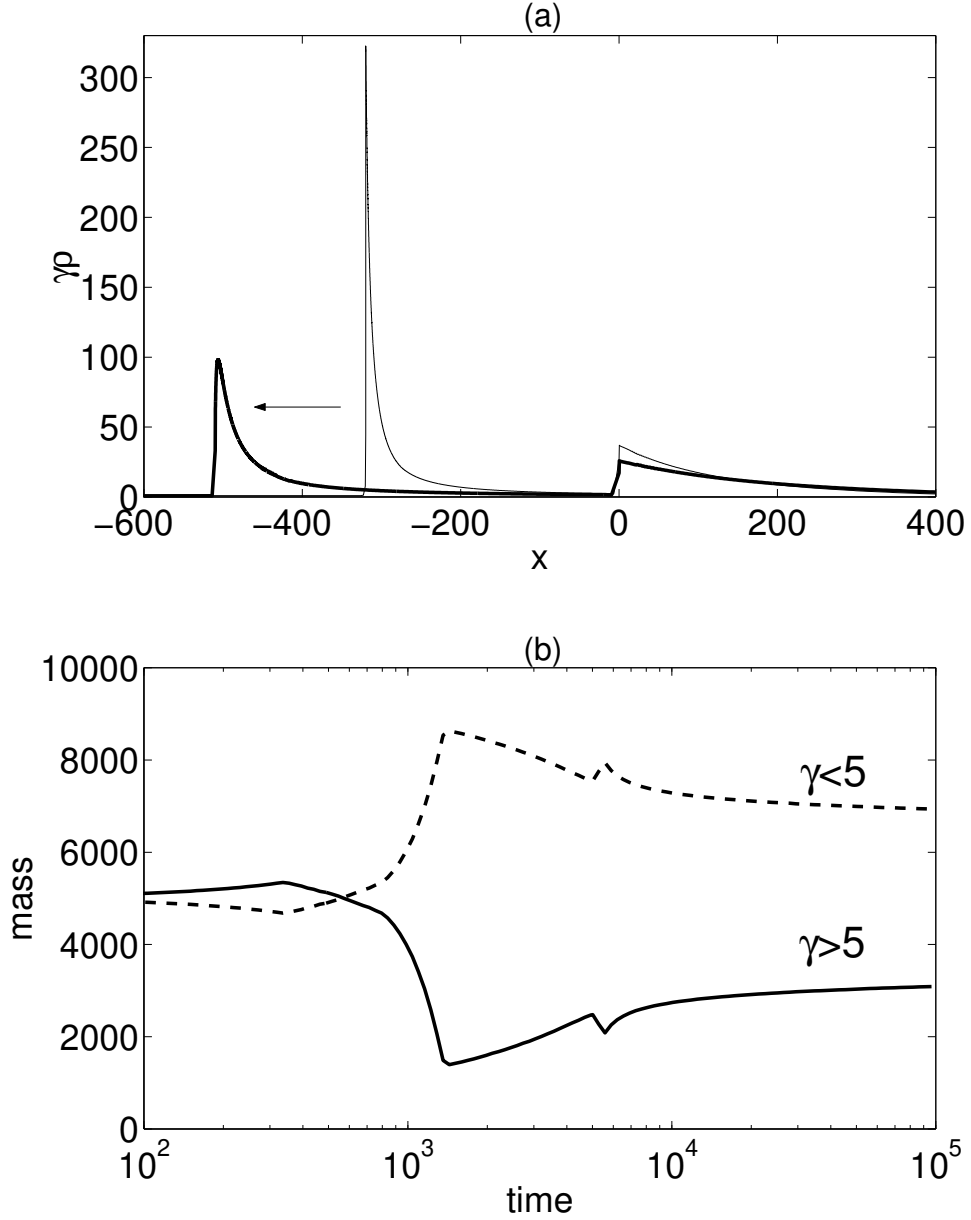


Fig. 2.— (a) Lorentz factor γ vs distance x from the contact surface at $t = 5000$ (thin) and 6000 (thick). The Lorentz factor γ and position x are measured in the rapid shell frame, and the density ρ is the the fluid local frame. (b) mass fractions: $\gamma > 5$ (solid) and $\gamma < 5$ (dashed)

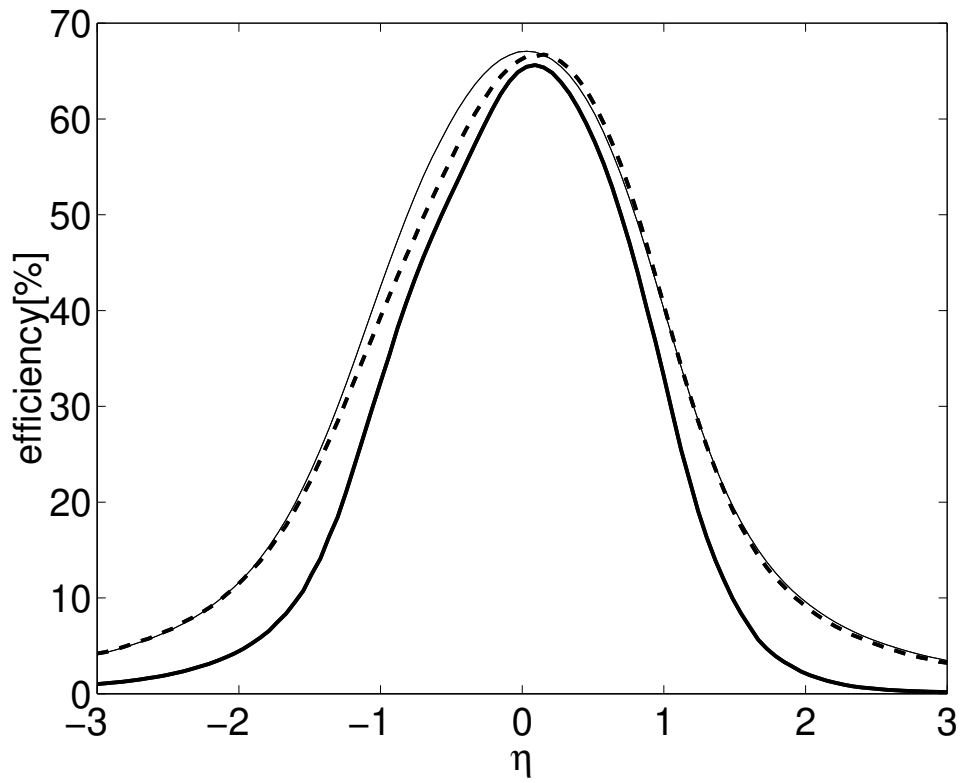


Fig. 3.— The efficiency is plotted as a function of η for different δ . $\delta = 0$ (thick solid), 0.4 (dashed) or 0.8 (thin). $N = 30$, $\gamma_{min} = 10$, $\gamma_{max} = 10^4$ and $\epsilon_e = 0.5$.

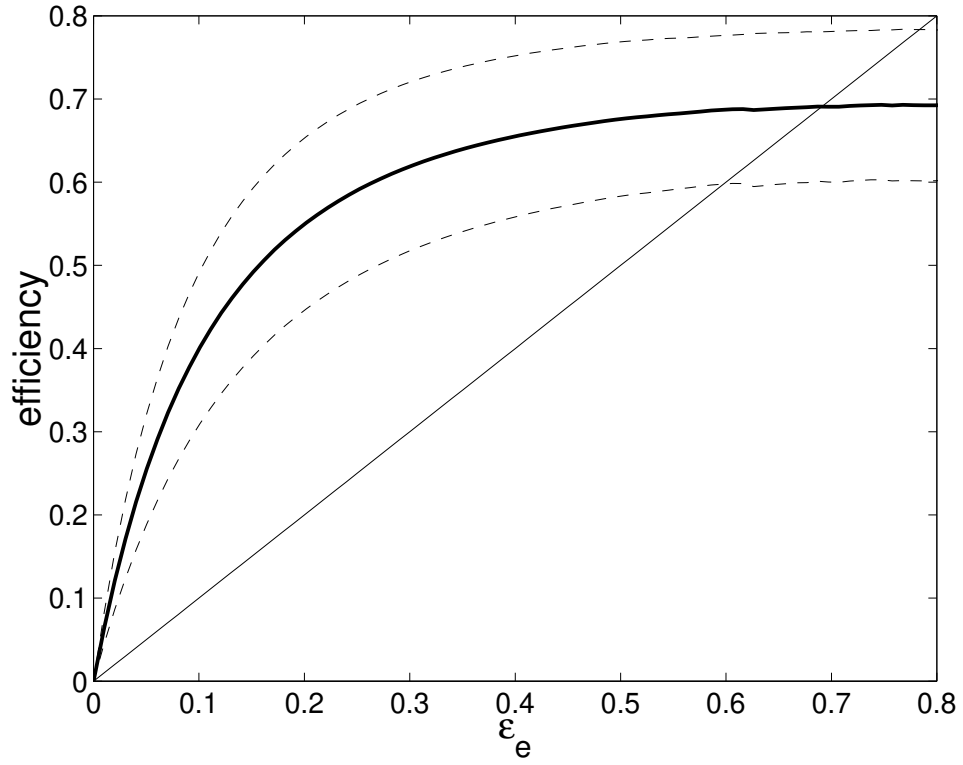


Fig. 4.— Efficiency vs ϵ_e with 1σ error bars of 100 random simulations. $N = 30$, $\eta = \delta = 0$, $\gamma_{min} = 10$ and $\gamma_{max} = 10^4$.

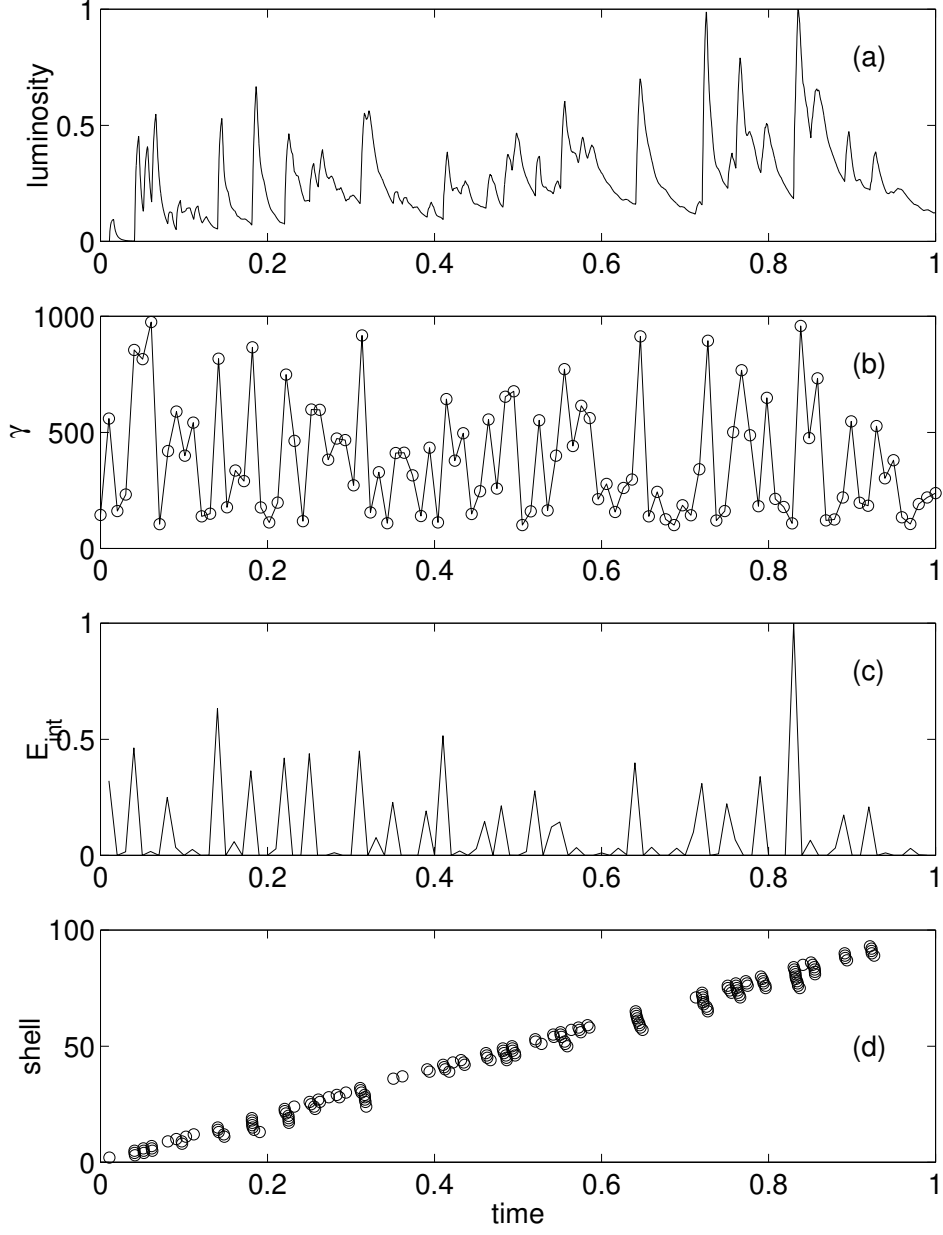


Fig. 5.— Temporal structure. (a) Numerical temporal structure. (b) Lorentz factor of a shell at the ejection vs ejection time (c) E_{int} between neighbor boring shells vs ejection time (d) Index of a shell vs observed time of the radiation produced in that shell. $N = 100$, $\gamma_{min} = 10^2$, $\gamma_{max} = 10^3$, $\eta = \delta = 0$ and $\epsilon_e = 0.1$.

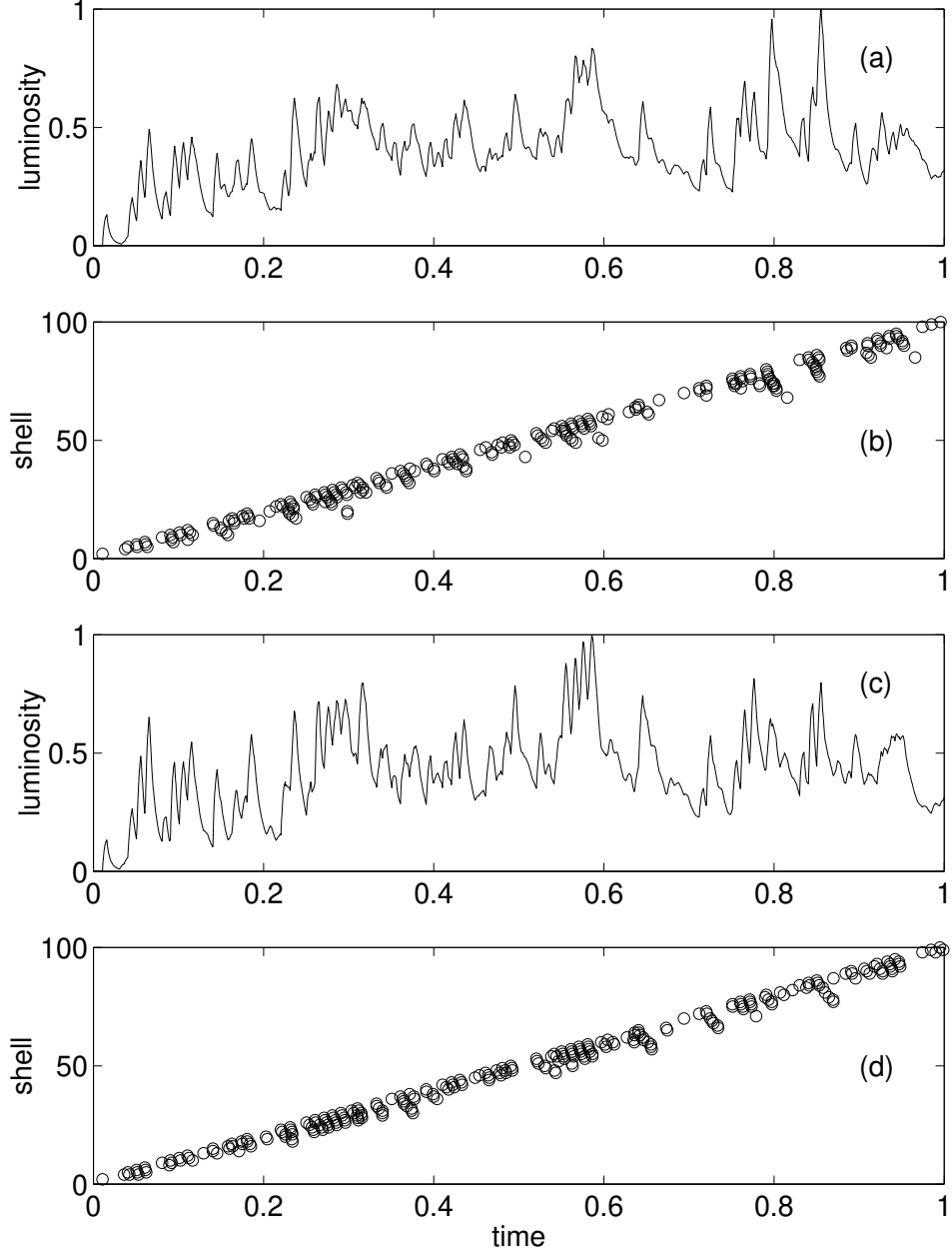


Fig. 6.— Temporal structure and correlation between the index of shell and the radiation observed time. The merger at each collision is assumed to split to the original masses (a and b) or to the modified masses with $\delta = 0.4$ (c and d). $N = 100, \eta = -1, \gamma_{min} = 10^2$ and $\gamma_{max} = 10^3$ and $\epsilon_e = 0.1$.